DINAME 2017 - Proceedings of the XVII International Symposium on Dynamic Problems of Mechanics
A. T. Fleury, D. A. Rade, P. R. G. Kurka (Editors), ABCM, São Sebastião, SP, Brazil, March 5-10, 2017

Identification of Rotordynamic Seal Coefficients by Means of Impedance Matrix and an Optimization Strategy

David J. G. M.[1], **Thiago G. R.**[2], **Fernando A. N. C. P.**[3]

[1] Department of Mechanical Engineering, Universidade Federal do Rio de Janeiro, Av. Horácio Macedo, 2030, Cidade Universitária, Rio de Janeiro - RJ, david.julian@ufrj.br, tritto@mecanica.ufrj.br, fcpinto@ufrj.br

Abstract: Theoretical modeling and experimental identification of annular seals parameters have been a challenge in the last 50 years due to the complex behavior of fluid inside these components. The complexity comes from the fluid dynamics that may create rotordynamic instabilities. A way to analyze instabilities in rotating machines with this kind of seals is by estimating the four main coefficients: direct stiffness and damping and cross-coupled stiffness and damping. For that reason, this paper presents and compares two methods to estimate seals coefficients using force and displacements measurements. The first method, the impedance matrix, uses position and force measurements at a fixed rotational speed of the machine to determine the seal matrix impedance. The real parts of the matrix are the stiffnesses and the imaginary parts the damping. On the other hand, the optimization method is based on a frequency sweep to compute the frequency response function (FRF), using position an force measurements. Then, an optimization algorithm is used to find the set of coefficients that best fits the experimental FRF. In the present stage of this research, only simulated data, with added Gaussian noise, is used to test the identification strategies.

Keywords: Annular Gas Seals, Identification Method, Matrix Impedance, Rotordynamics, Seal Coefficients

NOMENCLATURE

Latin symbols

C: damping matrix
K: stiffness matrix
M: mass matrix
G: gyroscopic matrix
ω: mode-shape frequency
u: displacement vector
f: force vector
t: time
$\mathbf{H}_i^{\text{exp}}$: experimental FRF
Z: Impedance matrix

Greek symbols

ν: mode-shape vector
ε: random error

Subscripts

x,y: x and y directions
xy,yx: cross-coupled directions
t: tangential direction
f: force
u: displacement

INTRODUCTION

Parameter identification is a relevant issue when analysing, designing and constructing machines. In the case of rotating machines, such as turbines, compressors and engines, two components are of special interest: bearings and seals. If the rotordynamic system can be linearized, these components reasonably modeled with mass, stiffness and damping elements. In the present paper only stiffeness and damping elements of seals are considered. These components are important to determine the stability of a rotating machine system. Different models and identification methods have been proposed in the literature (Childs, 1993, Ishida Yamamoto, 2013, Muszynska, 2005, Gasch et al., 2006).

An annular gas seal is a component used to maintain two regions at different pressures with minimum leakage, consequently there is a flow field inside the clearance. This flow and small variations of the clearance create forces (modeled as stiffness and damping elements). In the present modeling, the annular gas seal has four coefficients: direct stiffness and damping and cross-coupled stiffness and damping, which might be obtained exciting and measuring the rotordynamic system. Many methodologies of excitation have been proposed: impact hammer, shakers, magnetic actuators, active magnetic bearings, etc. Once the excitation and the system response have been measured, several identification strategies can be applied; see for instance Childs and Hale (1994), Picardo and Childs (2004), San Andrés (2003), Childs et al. (1989), Childs and Scharrer (1986), Lee et al. (2005), and Zhang et al. (2011). In the present paper, two identification strategies are applied: (1) the impedance matrix method (San Andrés, 2003) and (2) an optimization method proposed herein.

This paper is organized as follows. In Section a rotordynamic model discretized by means of the Finite Element Method (FEM) is presented. The Frequency Response Function (FRF) and Campbell function are analyzed. In Section

the identification strategies are depicted. In the optimization method, experimental data will be simulated and, by using an Levenberg-Marquadt algorithm, optimal set of coefficients are obtained minimizing the objective function. In the other method, a system matrix impedance, which contains the seal coefficients, is obtained in terms of the measurements. Finally, the conclusions are made in the last section.

FINITE ELEMENT ROTORDYNAMIC MODEL

The rotordynamic system under analysis is composed of a flexible shaft, two bearings and two annular seals. Figure 1 shows a sketch of the shaft, and it contains all the important dimensions. This test rig was built in LAVI (Laboratory of Acoustics and Vibration) in the Federal University of Rio de Janeiro, but, unfortunately, we do not have experimental data yet. The finite element representation of the system is obtained using the LAVIRot (Deus, 2015, Oliveira, 2016), developed by LAVI (Laboratory of Acoustics and Vibration). Each element is modeled as a Euler-Bernoulli beam theory, which considers 4-DOF for each element (two displacements and two rotations). Two ball bearings 6304-2Z were used as illustrated in Figure 2. The excitation signal is applied by two magnetic actuators shown in Figure 2. Two tooth-on-stator labyrinth seals are mounted symmetrically as shown in Figure 2. The final rotordynamic model is shown in Equation 1.

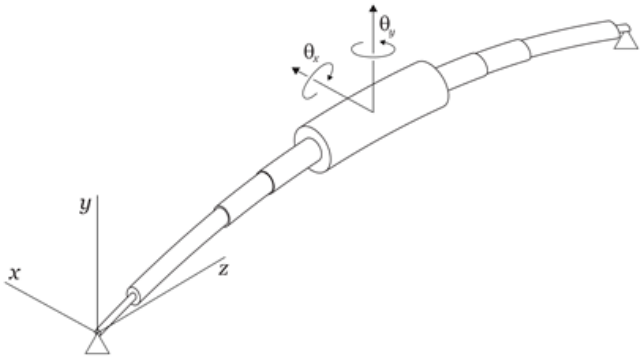

Figure 1: Finite-element rotor model

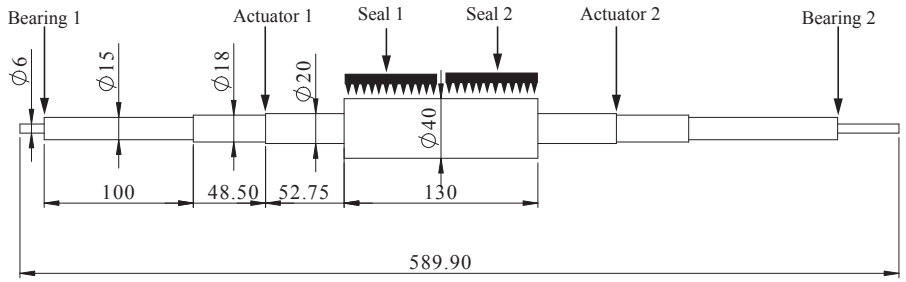

Figure 2: Dimensions of the shaft and location of the bearings (b_1 and b_2) and seals (s_1 and s_2)

$$\mathbf{M}\ddot{\mathbf{u}}(t)+(\mathbf{C}+\mathbf{G})\,\dot{\mathbf{u}}(t)+\mathbf{K}\mathbf{u}(t)=\mathbf{f}(t) \tag{1}$$

where $\mathbf{M}$ is the mass matrix, $\mathbf{C}$ is the damping matrix, $\mathbf{G}$ is the gyroscopic matrix, $\mathbf{K}$ is the stiffness matrix, $\mathbf{f}(t)$ is the external force vector and $\mathbf{u}(t)$ is the generalized displacement vector.

Each seal is modeled as a bi-dimensional spring-damper system with the following constitutive equation:

$$\begin{bmatrix}-f_x\\-f_y\end{bmatrix}=\begin{bmatrix}K_{xx} & K_{xy}\\K_{yx} & K_{yy}\end{bmatrix}\begin{bmatrix}u_x\\u_y\end{bmatrix}+\begin{bmatrix}C_{xx} & C_{xy}\\C_{yx} & C_{yy}\end{bmatrix}\begin{bmatrix}\dot{u}_x\\\dot{u}_y\end{bmatrix} \tag{2}$$

where, K_{xx}, C_{xx}, K_{yy}, C_{yy} are the direct stiffnesses and damping and K_{xy}, C_{xy}, K_{yx}, C_{yx} are the cross-coupled stiffnesses and damping.

The frequency model of Equation 1 is obtained by considering forces and displacement with the following harmonic behavior:

$$\begin{aligned}\hat{\mathbf{f}}(\omega) &= \mathbf{f}_0 e^{-j\omega t}\\ \hat{\mathbf{u}}(\omega) &= \mathbf{u}_0 e^{-j\omega t}\end{aligned} \tag{3}$$

Using Equation 3 in 1 yields the following frequency-domain model:

$$\left(-\omega^2\mathbf{M}+i\omega\left(\mathbf{C}+\mathbf{G}(\omega)\right)+\mathbf{K}\right)\hat{\mathbf{u}}=\hat{\mathbf{f}} \tag{4}$$

Frequency Response Function

The behavior of the rotor-bearing system can be analyzed using the FRF, which is defined in Equation 5.

$$\mathbf{H} = \left(-\mathbf{M}\omega^2 + (\mathbf{C} + \mathbf{G}(\omega))\, i\omega + \mathbf{K}\right)^{-1} \tag{5}$$

Figure 3 shows a simulation of a FRF calculated at the seal location (middle of the rotor). It shows the amplitude of the transversal oscillation as the speed of rotation increases. The two peaks seen in the figures are of special relevance since they are related to the natural frequencies of the system.

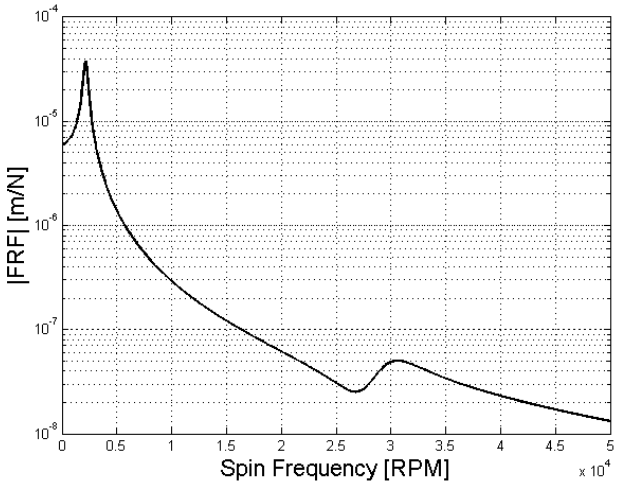

Figure 3: Frequency response function

Campbell Diagram

Another tool to analyze the frequency system behavior is the Campbell Diagram, which shows the frequency of each mode shape at different shaft speeds. In order to obtain the diagram, the following no forcing space-state representation is used:

$$\begin{bmatrix} \dot{\hat{\mathbf{u}}} \\ \ddot{\hat{\mathbf{u}}} \end{bmatrix} = \begin{bmatrix} \mathbf{0} & \mathbf{I} \\ -\mathbf{M}^{-1}\mathbf{K} & -\mathbf{M}^{-1}(\mathbf{C} + \mathbf{G}(\omega)) \end{bmatrix} \begin{bmatrix} \hat{\mathbf{u}} \\ \dot{\hat{\mathbf{u}}} \end{bmatrix} \tag{6}$$

Equation 6 yields the following eigenvalue problem:

$$\mathbf{A}v = \omega_k v \tag{7}$$

where ω_k is the frequency of the kth mode shape. A simulation of a Campbell Diagram is shown in Figure 4. This diagram shows the frequency of each mode shape (ω) as the speed of rotation (Ω) increases from 0 to 50000 RPM. At $\Omega = 0$, the three first natural frequencies can be seen in the vertical axis. When increasing Ω, each frequency splits into 2 lines: the forward and backward whirl. The dotted line shows the line $\omega = \Omega$, which intercept with the whirls correspond to the critical speeds. As was seen in Figure 3, there are 2 peaks that correspond to critical speeds. Only two peaks appear in Figure 3 because the second mode shape of the system has a node at the middle of the shaft.

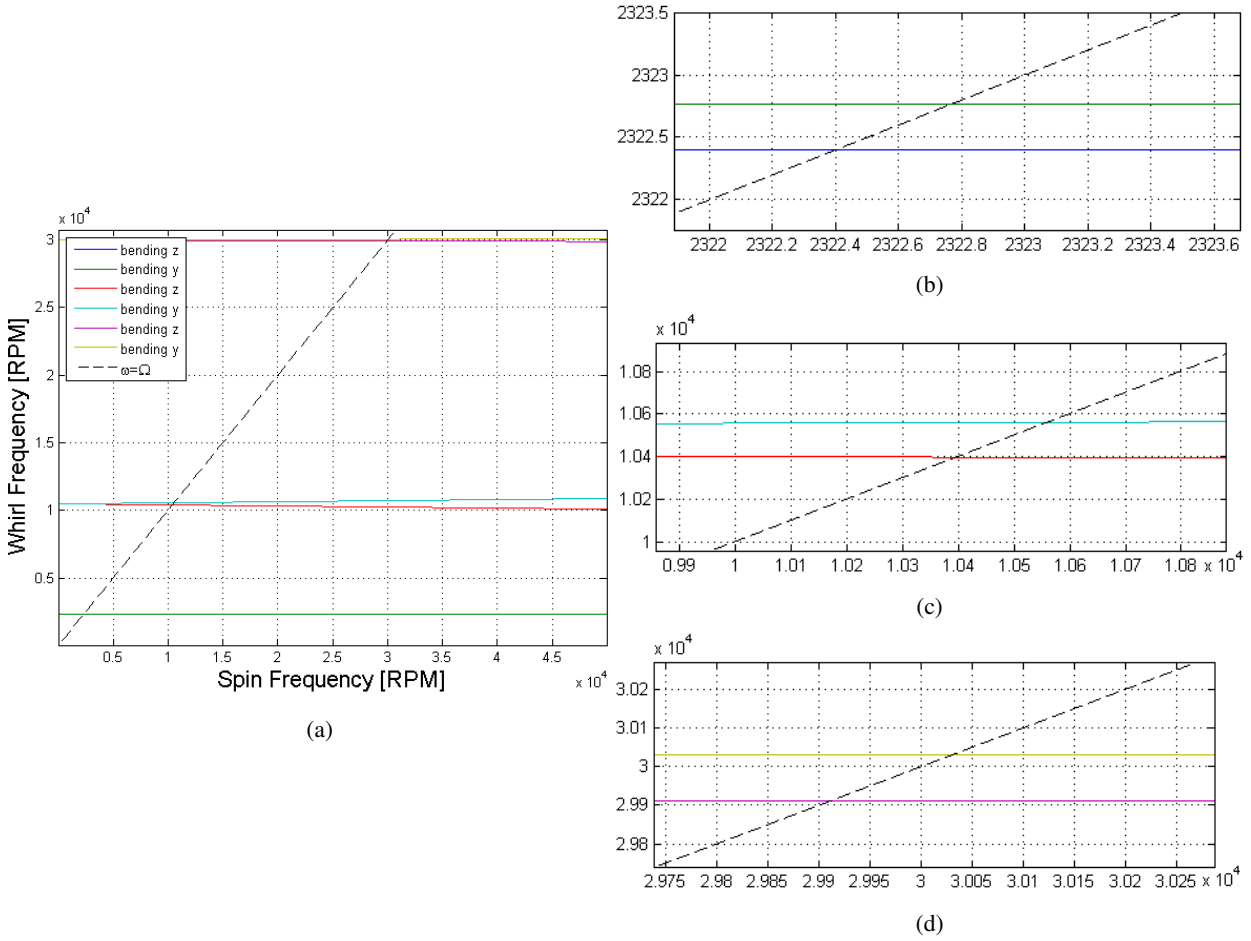

Figure 4: (a) Campbell Diagram of the first 3 critical speeds. (b) Forward and backward whirl of first critical speed. (c) Forward and backward whirl of second critical speed. (d) Forward and backward whirl of third critical speed.

IDENTIFICATION METHODS

In this section two identification methods to estimate the rotordynamic coefficients that appear in Equation 8 are presented. This set of coefficients were chosen assuming $K_{xx} = K_{yy}$, $K_{xy} = -K_{yx}$, $C_{xx} = C_{yy}$ and $C_{xy} = -C_{yx}$.

$$\mathbf{p}_k = \begin{bmatrix} K_{xxk} & K_{xyk} & C_{xxk} & C_{xyk} \end{bmatrix}, k = \{1,2\} \tag{8}$$

In order to obtain a response that includes the effects of all the coefficients, an external excitation is applied to the system. This can be done by using magnetic actuators, magnetic bearings, shakers or unbalancing disks. The force of these component can be modeled using Equation 3.

Optimization Strategy

This method is based on a minimization of a objective function involving an experimental and a theoretical FRF. The objective function $S(\mathbf{p})$ is defined in Equation 9.

$$S(\mathbf{p}) = \sum_{i=1}^{n} \left(\mathbf{H}_i^{\exp}(\Omega_i) - \mathbf{H}(\Omega_i, \mathbf{p})^{\text{ref}} \right)^2 \tag{9}$$

where $\mathbf{H}_i^{\exp}(\Omega_i)$ is the experimental FRF, $\mathbf{H}(\Omega_i, \mathbf{p})^{\text{ref}}$ is the analytical FRF in terms of the parameters $\mathbf{p}$ and Ω_i is the rotation speed or spin. The optimal set of parameters is reached when $S(\mathbf{p})$ is minimum, i.e., the error between the two responses has its minimum value. This optimization is based on a Levenberg-Marquadt algorithm (Moré, 1977).

Impedance Matrix

This method uses the seal position measurements, external force measurements and a rotordynamic model of the shaft and bearings (San Andrés, 2003). The model is the impedance matrix $\mathbf{Z}$ shown in Equation 10.

$$\mathbf{Z} = \left(-\omega^2 \mathbf{M} + i\omega \left(\mathbf{C} + \mathbf{G}(\omega) \right) + \mathbf{K} \right) \tag{10}$$

This model contains the seals impedance, which can be obtained using Equation 11, where $\hat{\mathbf{f}}_{k1}$ and $\hat{\mathbf{f}}_{k2}$ are the forces

applied at the seal, $\hat{\mathbf{u}}_{k1}$ and $\hat{\mathbf{u}}_{k2}$ are the seal displacements.

$$\mathbf{Z}_k = \begin{bmatrix}\hat{\mathbf{f}}_{k1} & \hat{\mathbf{f}}_{k2}\end{bmatrix}\begin{bmatrix}\hat{\mathbf{u}}_{k1} & \hat{\mathbf{u}}_{k2}\end{bmatrix}^{-1} = \begin{bmatrix}K_{xx}+i\omega C_{xx} & K_{xy}+i\omega C_{xy}\\ K_{yx}+i\omega C_{yx} & K_{yy}+i\omega C_{yy}\end{bmatrix} \quad k = \{1,2,...\} \tag{11}$$

Thus, each seal coefficient is obtained by taking the real and imaginary part of $\mathbf{Z}_k$. Note that matrix $\mathbf{Z}$ is valid for a single rotation speed Ω.

RESULTS

Optimization Method

This method is tested by using a simulated FRF with added Gaussian noise. The noise, considered to be present in the proximity sensors, is modeled as follows:

$$\tilde{\mathbf{H}}_s = \mathbf{H}_s + \tilde{\varepsilon}_H \tag{12}$$

where $\tilde{\varepsilon}_H$ is a normally distributed random variable with zero mean and standard deviation $\sigma_H = 2 \cdot 10^{-8}$m/N. This simulated data is used as input of the identification method (Figure 5a). The result of this method is shown In Figure 5b, where the green curve is the initial FRF, the red curve is the experimental FRF and the blue curve is the estimated FRF. Although experimental data are affected by noise, the method found a set of coefficients that best fit the curve. In Figure 6 is shown the simultaneous evolution of each coefficient and, at iteration 200, the optimal set of coefficient are found. In Table 1 is shown the comparison between the estimated and exact coefficients values. As the method is tested with noise, it was executed 200 times and the mean was chosen as an estimator of the coefficients values. These results show a minimum error of 2.69 %, for C_{xx}, and a maximum error of 44.84 %, for C_{xy}.

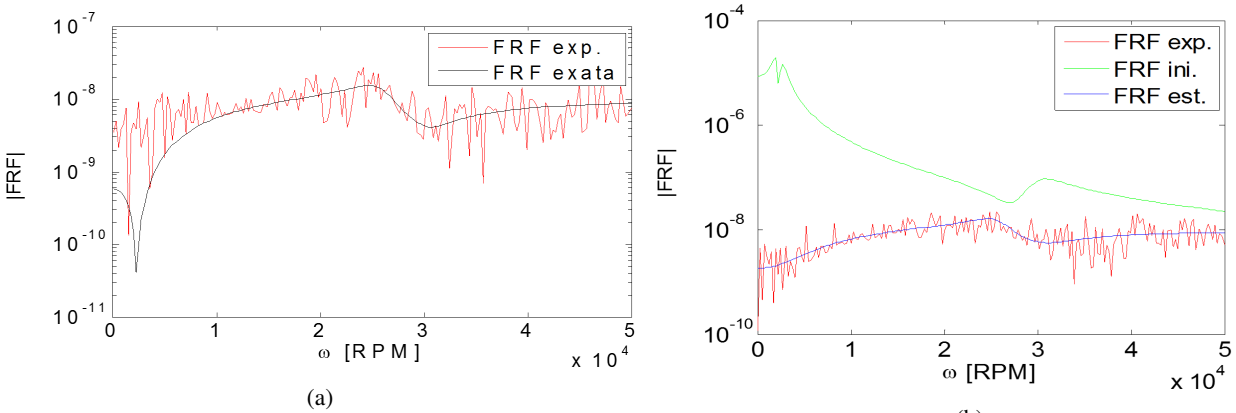

(a) (b)

Figure 5: (a) exact and experimental FRF. (b) Experimental, initial and estimated FRF.

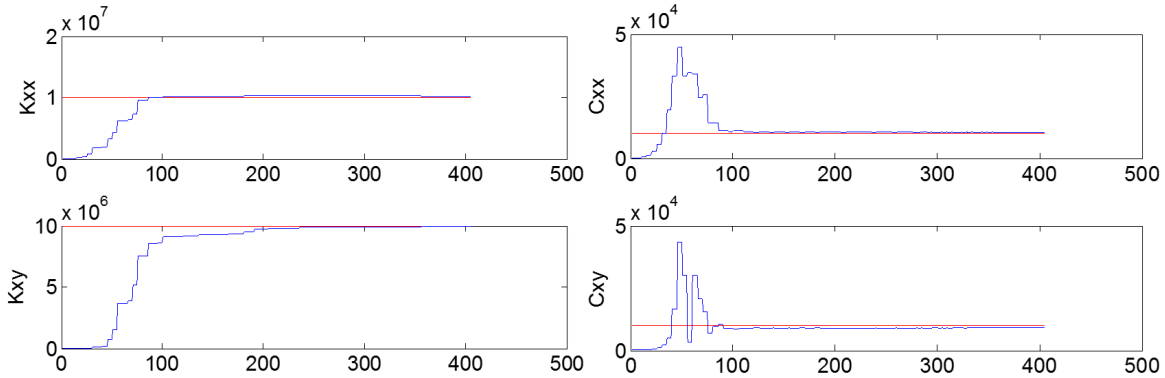

Figure 6: Evolution of the coefficients values through iterations

Coefficient	Estimated Value	Reference Value	Error
			%
K_{xx}	$1.224 \cdot 10^7$ N/m	10^7 N/m	22.45
K_{xy}	$8.535 \cdot 10^7$ N/m	10^7 N/m	14.65
C_{xx}	$1.027 \cdot 10^4$ Ns/m	10^4 Ns/m	2.69
C_{xy}	$5.516 \cdot 10^3$ Ns/m	10^4 Ns/m	44.84

Table 1: Results of the Optimization Method

Impedance Matrix

This method is tested with the same simulated experimental displacement vector from Equation 12, considering random values from proximity sensors. Thus, the impedance matrix from Equation 11 becomes:

$$\mathbf{Z}_{sk} = \begin{bmatrix} \hat{\mathbf{f}}_{k1} & \hat{\mathbf{f}}_{k2} \end{bmatrix} \begin{bmatrix} \hat{\mathbf{u}}_{k1} + \tilde{\varepsilon}_{k1} & \hat{\mathbf{u}}_{k2} + \tilde{\varepsilon}_{k2} \end{bmatrix}^{-1} \tag{13}$$

where $\tilde{\varepsilon}_{k1}$ and $\bar{\varepsilon}_{k2}$ are normally distributed random variables with zero mean and standard deviations $\sigma_u = 5 \cdot 10^{-7}$ m. In order to make a comparison to the previous method, the two standard deviation are equal but expressed in different units. The results are compiled in Table 2 with the estimated value, exact value and error. These method was also executed 200 times and a mean was chosen as an estimator of the coefficient value. The results showed a minimum error of 3.40 %, for K_{xy} and a maximum error of 8.60 %, for C_{xy}, which is less than the optimization method. These results were computed with a rotation speed of 15000 RPM.

Coefficient	Estimated Value	Reference Value	Error
			%
K_{xx}	$1.044 \cdot 10^7$ N/m	10^7 N/m	4.40
K_{xy}	$1.034 \cdot 10^7$ N/m	10^7 N/m	3.40
C_{xx}	$1.062 \cdot 10^4$ Ns/m	10^4 Ns/m	6.20
C_{xy}	$1.086 \cdot 10^4$ Ns/m	10^4 Ns/m	8.60

Table 2: Results of the Impedance Matrix Method

CONCLUSIONS

The two methods presented were able to identify the seals coefficients of a rotodynamic system with an acceptable error. This error was due to a simulated noise added to the exact displacements for each method.

The method of the optimization strategy required a transverse excitations with actuators and two displacement measurements per seal. The system FRF is calculated in a frequency band of interest and then compared with the exact model via Levenberg-Marquadt. This FRF implies a frequency sweep over the band. The method estimated the parameters with a maximum error of 44.84%.

The impedance matrix method also required a transverse excitation and displacement measurements. However, it was not necessary to realize a frequency sweep as the method estimates the parameters for a certain excitation and rotation speed. This method estimated the parameters with a maximum error of 8.60%.

The impedance matrix method performed better and it runs faster (<1s) than the optimization method (<2min). But the results of the impedance methods were obtained for only one specific shaft rotarion. Since there are no sufficient results to demonstrate the validity of the proposed methodologies, more investigation is required.

BIBLIOGRAPHY

Childs, D., Elrod, D., and Hale, K. (1989). Annular honeycomb seals: Test results for leakage and rotordynamic coefficients; comparisons to labyrinth and smooth configurations. Journal of Tribology, 111(2), 293–300.

Childs, D. and Hale, K. (1994). A test apparatus and facility to identify the rotordynamic coefficients of high-speed hydrostatic bearings. Journal of tribology, 116(2), 337–343.

Childs, D. W. (1993). Turbomachinery Rotordynamics: Phenomena, Modeling, and Analysis. John Wiley and Sons.

Childs, D. W. and Scharrer, J. K. (1986). Experimental rotordynamic coefficient results for teeth-on-rotor and teeth-onstator labyrinth gas seals. Journal of engineering for gas turbines and power, 108(4), 599–604.

Deus, P. A. L., (2015). Development of a Graphical User Interface for Simulation of Rotating Machinery, Focusing on the Influence of Labyrinth Seals in Structural Dynamics. Undergraduate Thesis in Mechanical Engineering.

Gasch, R., Nordmann, R., and Pfützner, H. (2006). Rotordynamik. Springer-Verlag. Ishida, Y. and Yamamoto, T. (2013). Linear and Nonlinear Rotordynamics: A Modern Treatment with Applications. John Wiley and Sons.

Lee, Y. B., Shin, S. K., Ryu, K., Kim, C. H., and Jang, G. (2005). Test results for leakage and rotordynamic coefficients of floating ring seals in a high-pressure, high-speed turbopump. Tribology transactions, 48(3), 273–282.

Moré, J.J., (1977) The Levenberg-Marquardt Algorithm: Implementation and Theory. Numerical Analysis, ed. G. A. Watson, Lecture Notes in Mathematics 630, Springer Verlag, pp. 105–116, 1977.

Muszynska, A. (2005). Rotordynamics. CRC Press. Picardo, A. and Childs, D. W. (2004). Rotordynamic Coefficients for a Tooth-on-Stator Labyrinth Seal at 70 Bar Supply Pressures: Measurements Versus Theory and Comparisons to a Hole-Pattern Stator Seal. Journal of Engineering for Gas Turbines and Power, 127(4), 843–855.

Oliveira, R. M., (2016). Numerical simulation of a rotor in test bench. Undergraduate Thesis in Mechanical Engineering.

San Andrés, L. (2003). A Method for Identification of Force Coefficients in Flexible Rotor-Bearing Systems. Research Progress Report to the Turbomachinery Research Consortium, TRC-B and C-2-03,

May. Zhang, W. F., Yang, J. G., Cao, H., and Sun, D. (2011). Experimental identification of fluid-induced force in labyrinth seals. Journal of mechanical science and technology, 25(10), 2485–2494.

RESPONSIBILITY NOTICE

The authors are the only responsible for the material included in this paper.